













Mutually inclusive mechanisms of drought-induced tree mortality

Peter Hajek¹  | Roman M. Link²  | Charles A. Nock^{1,3}  | Jürgen Bauhus⁴  |
Tobias Gebauer¹  | Arthur Gessler^{5,6}  | Kyle Kovach^{1,7}  | Christian Messier^{8,9} |
Alain Paquette⁸  | Matthias Saurer⁵  | Michael Scherer-Lorenzen¹  | Laura Rose¹  |
Bernhard Schuldt² 

¹Geobotany, Faculty of Biology, University of Freiburg, Freiburg, Germany

²Chair of Ecophysiology and Vegetation Ecology, University of Würzburg, Julius-von-Sachs-Institute of Biological Sciences, Würzburg, Germany

³Department of Renewable Resources, University of Alberta, Edmonton, Alberta, Canada

⁴Chair of Silviculture, University of Freiburg, Freiburg, Germany

⁵Forest Dynamics, Swiss Federal Institute for Forest, Snow and Landscape Research, Birmensdorf, Switzerland

⁶ETH Zurich, Institute of Terrestrial Ecosystems, Zurich, Switzerland

⁷Department of Forest and Wildlife Ecology, University of Wisconsin-Madison, Madison, Wisconsin, USA

⁸Center for Forest Research, Université du Québec à Montréal, Montréal, Quebec, Canada

⁹University of Quebec in Outaouais (UQO), Institut des Sciences de la Forêt Tempérée (ISFORT), Gatineau, Quebec, Canada

Correspondence

Peter Hajek, Geobotany, Faculty of Biology, University of Freiburg, Schänzlestr. 1, 79104 Freiburg, Germany.
Email: peter.hajek@biologie.uni-freiburg.de

Roman M. Link, Chair of Ecophysiology and Vegetation Ecology, University of Würzburg, Julius-von-Sachs-Institute of Biological Sciences, Julius-von-Sachs-Platz 3, 97082 Würzburg, Germany.
Email: roman.link@plant-ecology.de

Funding information

Deutsche Forschungsgemeinschaft, Grant/Award Number: 316733524 and 384026712; Schweizerischer Nationalfonds zur Förderung der Wissenschaftlichen Forschung, Grant/Award Number: 189109 and 310030

Abstract

Unprecedented tree dieback across Central Europe caused by recent global change-type drought events highlights the need for a better mechanistic understanding of drought-induced tree mortality. Although numerous physiological risk factors have been identified, the importance of two principal mechanisms, hydraulic failure and carbon starvation, is still debated. It further remains largely unresolved how the local neighborhood composition affects individual mortality risk. We studied 9435 young trees of 12 temperate species planted in a diversity experiment in 2013 to assess how hydraulic traits, carbon dynamics, pest infestation, tree height and neighborhood competition influence individual mortality risk. Following the most extreme global change-type drought since record in 2018, one third of these trees died. Across species, hydraulic safety margins (HSMs) were negatively and a shift towards a higher sugar fraction in the non-structural carbohydrate (NSC) pool positively associated with mortality risk. Moreover, trees infested by bark beetles had a higher mortality risk, and taller trees a lower mortality risk. Most neighborhood interactions were beneficial, although neighborhood effects were highly species-specific. Species that suffered more from drought, especially *Larix* spp. and *Betula* spp., tended to increase the survival probability of their neighbors and vice versa. While severe tissue dehydration

Peter Hajek and Roman M. Link contributed equally.

This is an open access article under the terms of the Creative Commons Attribution License, which permits use, distribution and reproduction in any medium, provided the original work is properly cited.

© 2022 The Authors. *Global Change Biology* published by John Wiley & Sons Ltd.

marks the final stage of drought-induced tree mortality, we show that hydraulic failure is interrelated with a series of other, mutually inclusive processes. These include shifts in NSC pools driven by osmotic adjustment and/or starch depletion as well as pest infestation and are modulated by the size and species identity of a tree and its neighbors. A more holistic view that accounts for multiple causes of drought-induced tree mortality is required to improve predictions of trends in global forest dynamics and to identify mutually beneficial species combinations.

KEYWORDS

carbon starvation, climate change, embolism resistance, hydraulic failure, IDENT, neighborhood interactions, non-structural carbohydrate dynamics, pest infestation, species mixture, tree mortality, TreeDivNet

1 | INTRODUCTION

Worldwide, most forested biomes are exposed to rises in temperature, atmospheric vapor pressure deficit and intensity and frequency of severe droughts (Dai, 2013; Yuan et al., 2019), resulting in large-scale tree dieback (Allen et al., 2015; Hammond et al., 2022). In the aftermath of extreme tree mortality events such as the 2018 summer drought in Central Europe (Peters et al., 2020; Schuldt et al., 2020), large forested areas rely on regeneration or reforestation with trees that have to be adapted to drier and/or hotter future climates. This underlines the urgent need for a more robust mechanistic understanding of the processes involved in drought-induced tree mortality in general (Brodribb et al., 2020; Choat et al., 2018) and the drought response of young and small trees in particular (Crouchet et al., 2019; van Mantgem et al., 2009; Nolan et al., 2021; Peng et al., 2011). Forecasting post-drought regeneration determines the structure and function of future forests and constitutes a key challenge to forest managers. Observations of mortality events in controlled experimental settings, therefore, constitute an excellent study object to observe mechanisms of drought-induced mortality and evaluate its impact on forest demographics to derive management strategies for climate change impacts.

Two interrelated physiological mechanisms are thought to be central for drought-induced tree mortality: hydraulic failure, which is the partial or complete loss of xylem functionality due to embolism formation, and carbon starvation driven by the depletion of non-structural carbohydrates (NSC, consisting of starch plus soluble sugars) due to negative drought impacts on photosynthesis (McDowell et al., 2008). Although there is clear evidence that hydraulic failure is a universal component of the processes preceding tree death under drought (Adams et al., 2017; Anderegg et al., 2016; Li et al., 2020; Nolan et al., 2021), the role of NSC reserves in these processes is still controversially debated (Adams et al., 2017; Blackman et al., 2019a; Kannenberg & Phillips, 2020; O'Brien et al., 2020). Both processes interact with biotic agent demographics (McDowell et al., 2008, 2011), as drought effects on the water and carbon balance may additionally predispose trees to pathogen or insect attacks (Hart et al., 2014; Huang et al., 2020),

exacerbating climate-driven forest mortality (McDowell et al., 2020; Seidl et al., 2017).

Past work on drought-induced mortality has identified a multitude of risk factors associated with drought-induced tree mortality (O'Brien et al., 2017). Specifically, *tree size* is often closely associated with individual mortality risk, although a higher drought vulnerability was both reported for tall adult trees that operate close to physical constraints for water transport (Bennett et al., 2015; Stovall et al., 2019) and for small trees with limited access to soil water reserves (Crouchet et al., 2019; van Mantgem et al., 2009; Nolan et al., 2021; Peng et al., 2011). Furthermore, water shortage may intensify interspecific tree *competition*, depending on species-specific patterns of water use strategies and above- and belowground niche partitioning (Ammer, 2019; Grossiord, 2019), thus affecting individual mortality risk via variation in local neighborhood composition (Fichtner et al., 2020; Vitali et al., 2018).

Recent studies have predominantly focused on one of the number of distinct mechanisms of drought-induced tree mortality and have documented responses of a variety of tree species from different biomes (Adams et al., 2017; Brodribb et al., 2020; Choat et al., 2018; O'Brien et al., 2017). Although such studies provide insights into emerging patterns, examining multiple mechanisms at play during tree death under drought is argued to be critical to advancing future process-based models of tree mortality (McDowell et al., 2019; Trugman et al., 2021). Consequently, field-based studies that jointly analyze multiple potential causes of drought-induced tree mortality across a range of functionally different tree species are urgently needed.

In 2018, Central Europe experienced an extreme summer drought, followed by a non-typical dry winter and spring. This global-change type drought event resulted in the highest average growing season temperature and vapor pressure deficit ever recorded for this region (3.3°C and 3.2 hPa above the long-term average for the reference period from 1961 to 1990, respectively) and caused unprecedented drought-induced tree mortality in adult trees of several species (Schuldt et al., 2020). Aggravating this situation, millions of saplings planted over the past years were lost (Schuldt et al., 2020 and references therein). Similar patterns of high sapling mortality

following severe drought have been observed in Mediterranean climates (Herrero et al., 2013; Young et al., 2020).

To address the complexity of interrelated mechanisms behind drought-induced tree mortality, we used observations from 9435 young trees belonging to six angiosperm and six coniferous species from Europe and North America grown in a tree diversity and nutrient enrichment experiment established in 2013 in Central Europe (Wein et al., 2016). Based on a Bayesian hierarchical modeling approach, we predicted the individual mortality risk following the drought using data on hydraulic traits, carbon dynamics, pest infestation, tree height, and interactions with neighboring trees. We examined (i) how hydraulic traits and NSC dynamics shape a tree species' susceptibility to drought-induced mortality and (ii) how the probability of dying on the individual level is modulated by tree height and the influence of biotic and abiotic factors.

2 | MATERIAL AND METHODS

2.1 | Study site

The data set for this study was collected in 2018/2019 in Freiburg, Germany (48°01'10"N, 7°49'37"E; 240 m a.s.l.). The study site has a mean annual temperature of 11.6°C and a mean annual precipitation of 881.8 mm (long-term average from 1989 to 2019). In the wake of the exceptionally hot and dry conditions that affected large parts of Central Europe in 2018 (Schuldt et al., 2020), the study site was subjected to the most severe summer drought ever recorded in the region. The mean temperature from June to August in 2018 was 2.0°C above (20.9 vs. 18.9°C) and precipitation rates 62% below (118.2 vs. 314.2 mm) the long-term average from 1961 to 1990, respectively (DWD Climate Data Center, 2020).

The experiment, part of the International Diversity Experiment Network with Trees (IDENT; Tobner et al., 2014) and a global network of tree diversity experiments (TreeDivNet; Paquette et al., 2018), is focused on effects of species richness, functional diversity and variation in resources, and uses high planting density to accommodate multiple gradients. The study site comprises 415 plots of 13 m², each containing 7 × 7 = 49 trees planted on a 0.45 m × 0.45 m grid, resulting in a total of 20,335 trees. A buffer zone of 0.9 m separates neighboring plots. The experiment manipulates tree diversity (richness: monocultures and two, four, six species; functional diversity: mixtures of varying similarity in functional traits), geographic origin (European, North American), and species composition (different species mixtures per diversity level) in a factorial randomized block design with four replicate blocks, using a species pool of six congeneric species pairs native to North America and Europe (Table 1). Mixtures comprising European species (with the exception of 6-species mixtures) were replicated for a tree species richness × fertilization sub-experiment with nitrogen (100 kg ha⁻¹ yr⁻¹), phosphorus (50 kg ha⁻¹ yr⁻¹) and N + P addition, respectively. All trees were planted in 2013 as 1–3 years old saplings on shallow sandy-loamy Cambisol (0.4 m) with a high gravel content bedrock (1.0 m). Details about the design can be found in Wein et al. (2016).

2.2 | Tree mortality and height

We surveyed the survival and health status of all 20,335 planted trees at pre-drought (2017/2018 inventory), directly after the drought in autumn 2018, and post-drought in early summer of 2019. In 2018, trees were classified as healthy, damaged (leaf browning or leaf loss), severely damaged (partial canopy dieback) or dead. In the census in 2019, which our model is based on, it was only recorded whether trees were alive, dead, or resprouted after death of the aboveground part of

TABLE 1 List of the 12 studied species

Acronym	Species	Origin	Group	Height (m)	Diameter (cm)
ACPL	<i>Acer platanoides</i> L.	EU	Angio	4.3 ± 1.4	3.3 ± 1.6
ACSA	<i>Acer saccharum</i> Marsh.	NA	Angio	4.7 ± 1.4	3.0 ± 1.0
BEPA	<i>Betula papyrifera</i> Marsh.	NA	Angio	4.9 ± 1.0	4.3 ± 1.4
BEPE	<i>Betula pendula</i> Roth.	EU	Angio	5.3 ± 1.2	5.0 ± 2.1
LADE	<i>Larix decidua</i> Mill.	EU	Gymno	3.8 ± 1.2	4.0 ± 1.7
LALA	<i>Larix laricina</i> (Du Roi) K. Koch	NA	Gymno	3.2 ± 1.2	2.8 ± 1.4
PIAB	<i>Picea abies</i> L.	EU	Gymno	2.1 ± 0.6	2.7 ± 0.7
PIPU	<i>Picea pungens</i> (Engelm.) var. <i>glauca</i>	NA	Gymno	1.2 ± 0.3	2.3 ± 0.7
PIST	<i>Pinus strobus</i> L.	NA	Gymno	2.5 ± 0.8	3.3 ± 1.0
PISY	<i>Pinus sylvestris</i> L.	EU	Gymno	2.7 ± 0.9	3.7 ± 1.5
QURO	<i>Quercus robur</i> L.	EU	Angio	2.2 ± 1.0	1.9 ± 1.1
QURU	<i>Quercus rubra</i> L.	NA	Angio	3.5 ± 1.5	2.4 ± 1.1

Note: Given are the acronyms, species names, origin (EU: Europe; NA: North America), group (angio- or gymnosperm), pre-drought tree height and stem diameter at 10 cm height (mean ± SD).

the tree (which we counted as dead, as the original stem was functionally dead in these cases). Our analysis was based on the subset of the inner 25 trees of each plot that were alive during the pre-drought inventory, resulting in a total of 9435 trees. These trees represent 90.9% of the 10,375 initially planted individuals in central positions. Because boreholes of the bark beetle *Pityogenes chalcographus* were observed on several trees in early July 2018, we additionally recorded the state of beetle infestation (bark beetles present/absent) for all conifers.

Pre-drought tree height (stem base to the apical branch) was measured during December 2017 and January 2018 for the 25 central trees of each plot as part of a yearly inventory. Additionally, a remote sensing campaign was carried out in July 2018 using a drone (Octo8XL, Mikrokopter GmbH, Saldenburg, Germany) equipped with an optical RGB camera with a 16-mm lens (Sony A5000, Stuttgart, Germany). The heights of the edge trees (for computation of neighborhood effects) were then imputed based on these remote-sensing derived aggregate and rescaled by the average height of the corresponding species in each plot to account for species differences (see Supplementary Material S1 for details).

2.3 | Hydraulic traits

For measuring xylem embolism resistance, 100–150 cm long branch samples were collected from 12–19 living trees per species with the exception of the two ring-porous *Quercus* species (3–5 trees \times 4 plots \times 10 species = 171 samples in total) in late summer 2019, immediately wrapped in moist towels and stored in black plastic bags to prevent dehydration during transport. Samples were recut under water directly before xylem vulnerability curves were constructed according to standard protocols for short-vesseled coniferous and diffuse-porous species using the flow-centrifuge technique (Cochard et al., 2005). Vulnerability curves were fitted in R v4.0.0 (R Core Team, 2020) with nonlinear least squares using a sigmoidal model based on the raw conductance measurements (Ogle et al., 2009) (see details in Supplementary Material S1). Values for the long-vesseled *Quercus* species were obtained from literature (Lobo et al., 2018). Midday leaf water potential (Ψ_{md} , MPa) was measured for four trees per species in all 48 monocultures at the peak of the drought (12–14 August, 2018) using a Scholander pressure chamber (1505D-EXP, PMS Instruments, Corvallis, USA). HSMs were computed as the difference between Ψ_{md} and averages of the critical xylem pressure (P_{crit}), which was assumed to be equivalent to the pressure at 88% loss of conductivity for angiosperms and 50% for conifers (Brodribb & Cochard, 2009; Urli et al., 2013). To account for the uncertainty in the estimated vulnerability curve parameters, this uncertainty was propagated into the calculated HSM values (see Supplementary Material S1).

2.4 | Non-structural carbohydrates

The change in relative sugar content (i.e., in the relative contribution of soluble sugars to the total non-structural carbohydrate content, TNSC)

over the course of a drought event can be expected to act as an indicator for the amount of starch-to-sugar conversion (He et al., 2020; Schönbeck et al., 2020). The latter is a process associated with osmotic adjustment as well as with starch depletion for respiratory needs, both of which indicate a metabolic response to adverse drought conditions. To monitor changes in NSC pools, leaf samples for the analysis of non-structural carbohydrate contents were taken during pre-drought (21 May to 18 June 2018) after leaf enfolding was completed in monocultures (48 plots), and post-drought (1–4 October 2018) on the full design. Sampling was conducted on three trees per plot, yielding ~1,000 sampled trees in total, which were pooled per plot and species for chemical analyses. Leaves were sampled from a random subset of the inner 5 \times 5 trees (representing the most common tree size) whenever possible, but buffer trees were sampled if less than three trees per species were available for sampling in the core area. Each three to five leaves or 50–100 needles from a vital branch of the upper and middle part of the canopy were pooled, immediately stored at 4°C in the field and, within the same day, oven-dried at 60°C for 48 h to stop enzymatic activity (Landhäusser et al., 2018).

The low-molecular-weight sugars (glucose, fructose, and sucrose) and starch were analyzed following the protocol of Wong (1990), modified according to Hoch et al. (2002) (see Supplementary Material S1 for details). The change in relative sugar content over the growing season (Δ_{sugar}) was then calculated as the difference in the percentage of soluble sugars measured in May and in October 2018 in 48 unfertilized plots in the monocultures as $\Delta_{sugar} = (\text{sugar/TNSC May}) - (\text{sugar/TNSC Oct})$ (see Figure S2.1 for raw NSC contents).

2.5 | Neighborhood effects

The influence of the up to eight immediate neighbor trees on each of i in I central trees was expressed in form of a $I \times J$ neighborhood matrix \mathbf{N} containing the sum of the heights h_j of the trees of species j of J species divided by the height h_i of the central tree, weighted by their relative distance d_{ij} (i.e., with a weight of 1 for first and $1/\sqrt{2}$ for second order neighbors; see Supplementary Material S1):

$$N_{ij} = \sum \frac{h_j}{h_i d_{ij}} \quad (1)$$

In this formulation, the computed value can be interpreted as a partial Hegyi competition index (Hegyi, 1974) for the corresponding neighbor species, thus effectively decomposing the contribution of different competitor species to the total neighborhood effect.

2.6 | Statistical modeling

In a hierarchical Bayesian modeling framework based on the Stan probabilistic programming language Stan v. 2.21.0 (Carpenter et al., 2017), we described the observed tree mortality status in 2019 as a function of the individual mortality risk.

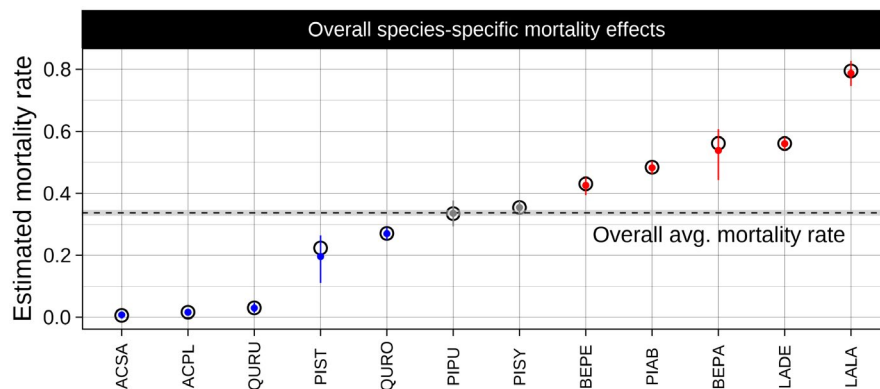


FIGURE 1 Average estimated mortality rates for each species ordered by magnitude (posterior mean \pm 95% highest posterior density interval [HDI]). Dashed line with grey ribbon: overall predicted average \pm 95% HDI. Red: risk credibly elevated over average level; blue: risk credibly below average; grey: not credibly different from average (based on 95% HDI). For species acronyms, see Table 1. Black circles: observed average mortality rates

We assumed that the observed state of a tree ($Y_{obs[ijk]}$; 0: tree alive, 1: tree dead) for each tree i belonging to species j in plot k for a total of I trees, J species and K plots is subject to observation errors with a species-specific probability of erroneously classifying a living tree as dead (e.g., because of leaf shedding). To account for this misclassification, we modeled the observed mortality state of individual trees as a one-inflated Bernoulli process with a tree-specific probability of dying p_{ijk} and a species-specific misclassification probability ϕ_j .

$$\Pr(Y_{obs[ijk]} = 0 | p_{ijk}, \phi_j) = (1 - \phi_j) \cdot (1 - p_{ijk}) \quad (2)$$

$$\Pr(Y_{obs[ijk]} = 1 | p_{ijk}, \phi_j) = \phi_j + (1 - \phi_j) \cdot (1 - p_{ijk}) \quad (3)$$

We further included observation models for the two species level traits in the focus of our main hypotheses, namely the *HSM* and Δ_{sugar} (see details in Supplementary Material S1).

We expressed the probability of dying p_{ijk} of each tree as a logit-linear function of the true species-level Δ_{sugar} and *HSM* values, a term specifying species-specific intercept and effects of tree height, bark beetle infestation and nutrient treatment ($I \times L$ predictor matrix X), a term specifying neighborhood effects ($I \times J$ neighborhood matrix N , elevated to a power of c), and species-specific plot effects δ_{jk} .

$$\text{logit}(p_{ijk}) = HSM_{true[j]} \cdot \alpha_{HSM} + \Delta_{sugar_{true[j]}} \cdot \alpha_{\Delta_{sugar}} + X_i \beta_j + N_i^c \gamma_j + \delta_{jk} \quad (4)$$

The $J \times L$ species-specific regression coefficients β were described by a multivariate normal distribution with covariance matrix Σ_β :

$$\beta_j \sim \text{MVN}(\beta_0, \Sigma_\beta) \quad (5)$$

To account for a possible correlation between the directed neighborhood effects within a pair of species, the $J \times J$ neighborhood effects matrix γ for focal species m and neighbor species n was parameterized as follows:

$$\begin{pmatrix} \gamma_{m,n} \\ \gamma_{n,m} \end{pmatrix} \sim \text{MVN} \left(\begin{pmatrix} \gamma_{0[n]} \\ \gamma_{0[m]} \end{pmatrix}, \tau_\gamma^2 \Omega_\gamma \right) \text{ for all } \gamma \text{ with } m \neq n \quad (6)$$

$$\gamma_{m,n} \sim \text{Normal}(\gamma_{0[n]}, \tau_\gamma) \text{ for all } \gamma \text{ with } m = n \quad (7)$$

where Ω_γ is a 2×2 correlation matrix allowing for a correlation of the directed neighborhood effects in pairs of non-identical species (the off-diagonal elements of γ).

The design effects δ for each plot and species were modeled by a normal distribution centered around zero with standard deviation τ_δ , that is, as a varying intercept for each combination of plot and species:

$$\delta_{jk} \sim \text{Normal}(0, \tau_\delta) \quad (8)$$

Modeling was performed via R using rstan v. 2.19.3 (Stan Development Team, 2020). The model reached a \hat{R} statistic of under 1.002 and effective sample sizes above 1500 for all estimated parameters, indicating full model convergence (Table S2.2). The estimated species-specific misclassification rates ϕ were low (on average 0.9%; Supplementary Material S1), although higher rates of up to 4.3% of trees erroneously classified as dead were found for some species (Table S2.2, Figure S2.2), resulting in a visible mismatch between observed and predicted mortality for these species in Figure 1. Details about model structure, prior specification, model implementation and model fitting are provided in Supplementary Material S1. The model code and raw data are available as a repository on Github (https://github.com/r-link/mutually_inclusive_mechanisms).

3 | RESULTS

3.1 | Interspecific variation in drought-induced tree mortality

In response to the severe drought of the year 2018 and the prolonged dry conditions that followed throughout the winter and spring of 2019, 34% of the 9435 trees present in our experimental plantation died. Tree mortality increased dramatically, given cumulative

mortality from 2013 to before the drought was 9% (see Section 2). Mortality over the period from 2017 to 2019 varied strongly across the 12 studied species, ranging from 0.6% for *A. saccharum* to 79.5% for *L. laricina* (Figure 1, Table S2.1). The average probability of dying predicted by our model (full output in Table S2.2) closely resembled the species-level mortality observed in the field (Figure 1) and explained 51.8% of the variance in the observed individual and 91.7% in the plot-level mortality (Figure 2). Mortality was elevated above the average mortality rate for *Larix* spp., *Betula* spp. and *P. abies*, whereas it was much lower than average specifically for *Acer* spp. and *Q. rubra* (below 10% in all three cases).

3.2 | Hydraulic safety margins and non-structural carbohydrates

Both hydraulic traits and carbohydrate dynamics differed considerably among species, with observed HSMs ranging from 0.63 to 3.65 MPa, and changes in the fraction of soluble sugars (glucose, fructose and sucrose) to total leaf NSC (Δ_{sugar}) over the growing season ranging from -33.2 to +17.0% (Figure 3). The observed differences in HSM and Δ_{sugar} were both strongly associated with species-level mortality risk, which was lower for species with a wider HSM and higher for species with a more pronounced increase in relative leaf sugar content over the vegetation period (Figures 3 and 4).

3.3 | Determinants of individual mortality risk

On the individual level, the species-specific mortality risk of a tree was modulated both by intrinsic variables and by interactions with the biotic and abiotic environment. Within species, there was a positive effect of tree height, resulting in a lower individual mortality risk for taller trees in all species except for *Q. rubra*, though the magnitude of that height effect varied strongly among species (Figure 4;

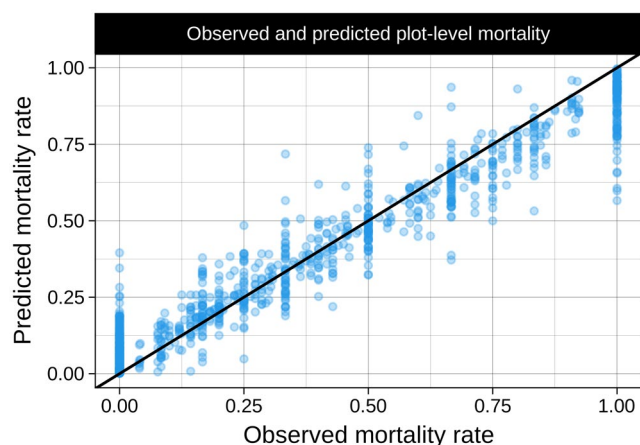


FIGURE 2 Posterior mean species-wise plot average mortality rate vs. observed proportion of dead trees per species and plot (explained variance in individual tree mortality: 51.8%; explained variance in species-wise plot averages: 91.7%)

Figure S2.3). In addition, individuals diagnosed with bark beetle infestation in 2018 had a much higher probability of dying (Figure 4). The prevalence of bark beetles differed greatly between species, with stronger outbreaks only for the native conifers *L. decidua* and *P. abies* (Table S2.1). Although the overall prevalence of bark beetle infestation was relatively low with 15.8 and 12.8% infested trees for *L. decidua* and *P. abies*, respectively, in both species infested individuals died with a high probability. The presence of bark beetles in neighboring trees had no overall effect on mortality (Figure 4), although on species level it was associated with higher mortality risk for *P. abies* (Figure S2.3), one of the two species with strong beetle infestation. None of the nutrient-enhancement treatments (N, P, or NP addition) affected mortality risk compared with the control treatment for any of the analyzed species (Figure 3, Figure S2.3). However, the variance explained by the species-wise plot effects (Figure S2.4, Figure S2.6) highlight systematic differences in mortality risk between plots and, hence, the presence of small-scale patterns driven by unobserved environmental variables.

3.4 | Neighborhood effects on mortality risk

Our model for neighborhood interactions captured the effect of the relative height of each of the eight immediate neighbor trees on the mortality risk of focal trees (Equation (1), Figure S1.1) while accounting for all possible inter- and intraspecific pairs of neighbor species. The number of neighbors of a particular species surrounding each focal tree varied depending on the species mixture in the plot and pre-drought background mortality. The presence of more and larger neighbors of a given species was associated with a reduced mortality risk for the focal tree in the majority of possible combinations, resulting in a negative overall neighborhood effect on the mortality risk of a focal tree for the majority of neighbor species (Figure 5a).

A. platanooides was the only species whose presence credibly increased the average mortality risk of its neighbors (Figure 5a). Across pairs of tree species, beneficial interactions were much more common than detrimental ones (Figure 5b). There was a tendency for interactions between neighbor species to be either one-sided or mutually beneficial, whereas not a single combination resulted in an increased mortality risk for both species (Figure S2.5). In general, species that suffered more from drought increased the survival probability of their neighbors and vice versa. Although *A. platanooides*, the species that most strongly increased the mortality of its neighbors, was among the species least affected by drought, four of the five species with positive effects on the survival of their neighbors suffered losses of more than 50% (Figure 1, Figure 5a). Besides an increased mortality risk of *P. pungens* in the neighborhood of *P. abies*, the only species that reduced the survival of any of their neighbor species were *A. platanooides* and *Q. rubra*. The presence of these two dominant overstory species increased the mortality especially for suppressed, subordinate species (Figure 5b).

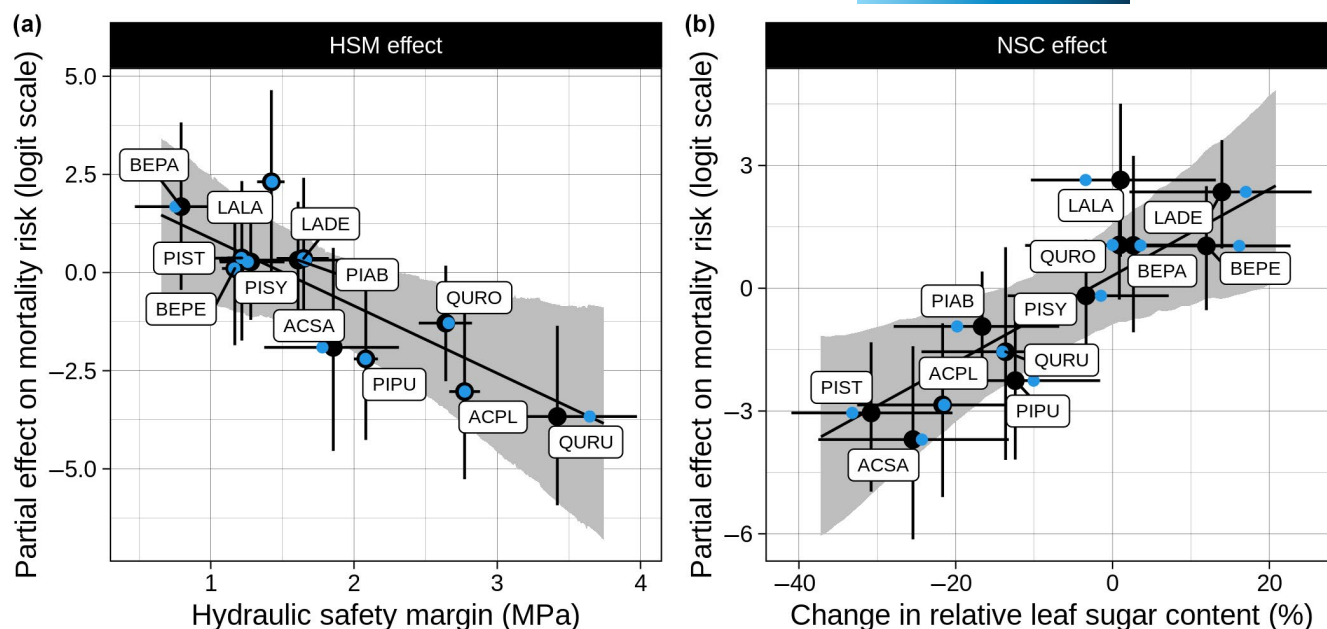
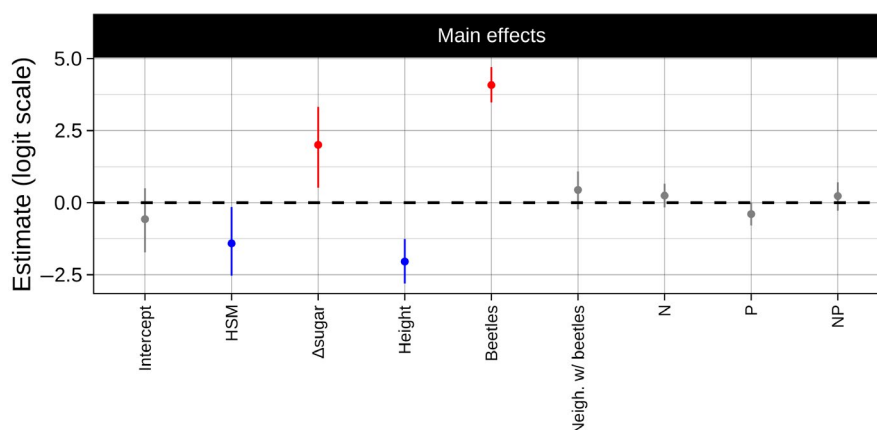


FIGURE 3 Partial effects for the species level effects of (a) hydraulic safety margins and (b) change in relative leaf sugar content (indicative of starch depletion) on mortality risk, i.e. the counterfactual predicted mortality risk for an average-sized, unfertilized, beetle-free tree without neighborhood effects while keeping. (a) Δ_{sugar} and (b) HSM at their overall average value. Black line with grey bands: posterior mean \pm 95% HDI. For species acronyms, see Table 1. Blue points: average observed values; black points: estimates \pm 95% HDI

FIGURE 4 Estimated main effects on mortality risk on the logit scale (posterior mean \pm 95% HDI). Blue: credibly reduced risk; red: credibly elevated risk; grey: no credible effect on mortality. HSM: hydraulic safety margins; Δ_{sugar} : change in sugar fraction of leaf NSC content. Compare Figure S2.3 for species-specific effects



4 | DISCUSSION

4.1 | Hydraulic failure or carbon starvation?

According to our model, species-level mortality risk was not only lower for trees with wider HSMs, but also strongly associated with changes in relative leaf sugar contents over the vegetation period, that is, the relative contribution of soluble sugars to total non-structural carbohydrates (Δ_{sugar}). The observed increase in Δ_{sugar} in more strongly drought-affected species is indicative of starch depletion and higher need of soluble sugars for osmotic adjustment (Hartmann et al., 2021; Thalmann & Santelia, 2017). Accordingly, drought-induced mortality risk in the studied species was jointly influenced by both variables associated with hydraulic failure and with

carbon starvation (McDowell et al., 2011; Mencuccini et al., 2015; Sapes et al., 2019).

The lower mortality we observed in species with wider HSM is in line with reported cross-species patterns in all forested biomes (Anderegg et al., 2016; Li et al., 2020; Powers et al., 2020; Trugman et al., 2021), and supports the hypothesis that hydraulic traits capture proximate mechanisms determining tree death (Adams et al., 2017). After the loss of hydraulic connectivity at the soil-root-interface during prolonged drought (Carminati & Javaux, 2020), the amount of internally stored water and its loss via leaky stomata, the cuticle and the bark determine the timing of lethal tissue dehydration (Blackman et al., 2016; Choat et al., 2018; López et al., 2021). Reaching critical desiccation thresholds inducing meristematic cell death (de la Mata et al., 2017; Guadagno et al., 2017; Mantova et al.,

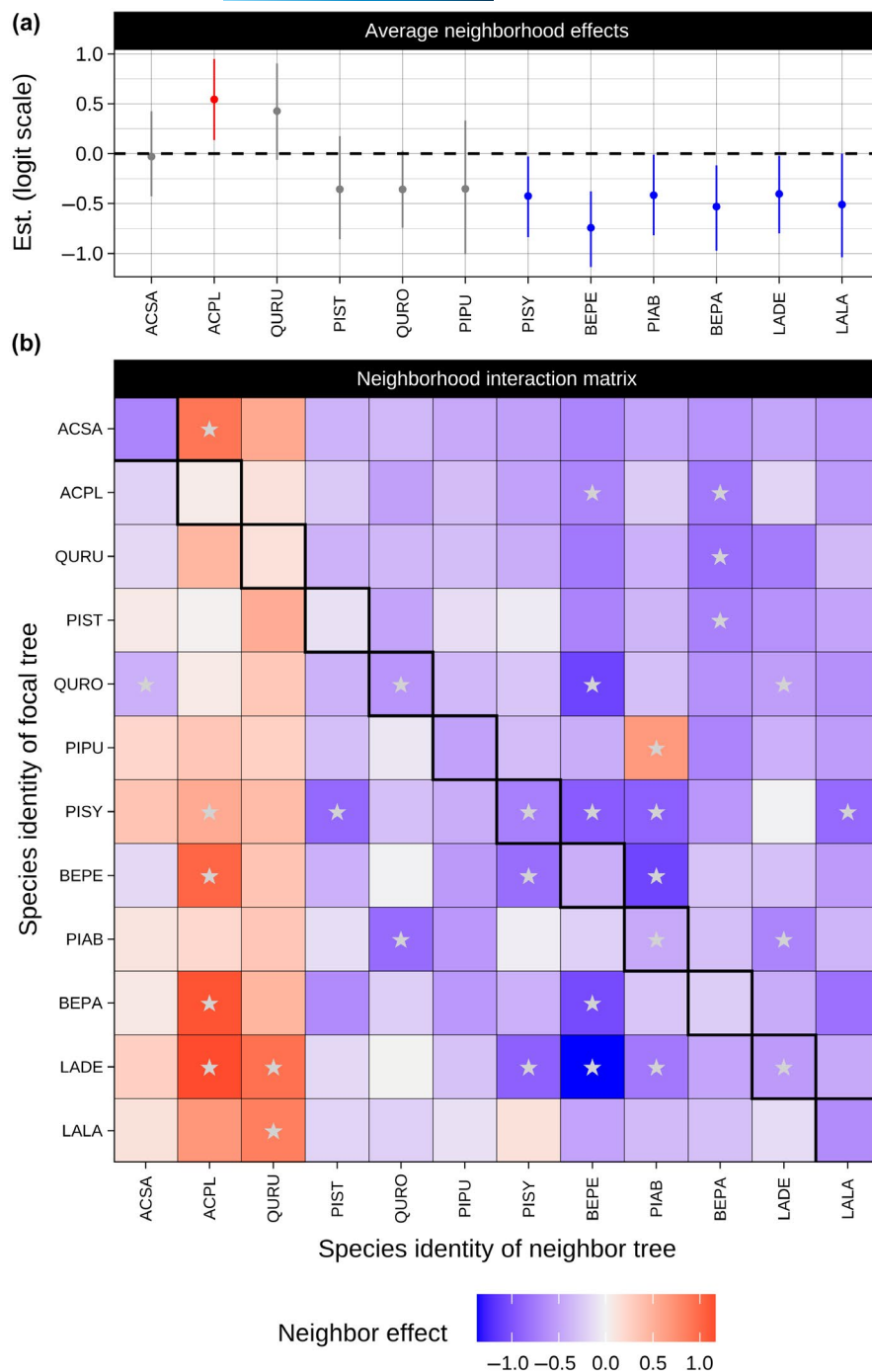


FIGURE 5 (a) Estimated average neighborhood effect; i.e. effect of a given neighbor species on the mortality risk of an average focal tree (shown are posterior mean \pm 95% HDI on the logit scale). Blue: credibly reduced risk; red: credibly elevated risk; grey: no credible effect on mortality. (b) Full matrix of the neighborhood effects of neighbors of a given species (columns) on focal trees of a target species (rows) on the logit scale. Colors indicate the strength of the effect (blue—reduced mortality risk, red—increased mortality risk); stars indicate effects that are credibly different from zero at the 95% level. The highlighted panels on the plot diagonal show intra-specific neighborhood effects. Species are ordered by increasing average mortality risk (cf. Figure 1). For species acronyms, see Table 1

2021) may, thus, mark the final step in the dying process of trees rather than being the cause of death.

The diverse physiological responses of NSC reserves at the time of death observed in previous studies indicate that, in contrast to hydraulic failure, carbon starvation is not a universal phenomenon of tree death during drought events (Adams et al., 2017; Hartmann et al., 2013). However, partial canopy dieback and/or the loss of xylem functionality will result in a reduction of leaf area, which in turn affects whole-plant net photosynthesis and carbon allocation in post-drought years. Moreover, recent evidence suggests that embolism repair under tension, that is, restoration of xylem functionality concurrent with transpiration, is either a rare phenomenon or even

completely absent in many tree species (Charrier et al., 2016; Choat et al., 2019; Rehschuh et al., 2020, but see Tomasella et al., 2021). This might explain commonly observed legacy effects of reduced vigor and increased mortality rates up to several decades after a drought event (Cailleret et al., 2017; Trugman et al., 2018), as well as different patterns of post-drought recovery (Li et al., 2020). The mechanisms governing drought-induced tree mortality and recovery might, therefore, be closely linked to carbon dynamics (Trugman et al., 2018). Noteworthy, *Larix* spp. and *Betula* spp., two of the most strongly drought-affected genera, showed signs of leaf browning and defoliation already in early July 2018. Although leaf shedding can mitigate drought effects on a plants' water balance via reduction

of the transpiring surface (Blackman et al., 2019b), the high Δ_{sugar} in these genera (Figure 3) indicates that the reduced carbon gain caused by this strategy may have contributed to their high mortality rates.

Both access to carbohydrate reserves and their utilization rate have been reported to be controlled by water availability (Sevanto et al., 2014), providing evidence that carbohydrate use is controlled by the functionality of the water transport system rather than by photosynthetic carbon gain. This is consistent with a hydraulic constraint on NSC consumption (McDowell et al., 2011; McDowell & Sevanto, 2010). The role of carbohydrates in osmotic adjustment constitutes a central link between carbon metabolism and hydraulic functioning (Hartmann et al., 2021; Pantin et al., 2013). Experimental manipulation of NSC storage has been shown to affect osmotic regulation and shift the turgor loss point towards substantially less negative water potentials even in the absence of drought (Sapes et al., 2021). This is consistent with a recent meta-analysis providing evidence for a decrease in starch and rise in soluble sugars over the course of extreme drought events (He et al., 2020). The observed decrease of the relative starch fraction in the more drought-affected species is a strong indication for starch-to-sugar conversion to meet the trees' metabolic and osmoregulatory demands during drought. The use of stored starch to produce osmotically active sugars indicates that the supply with recent assimilates was not sufficient for osmotic regulation. For example, extreme drought led to a strong conversion of starch to sugars in needles and other plant tissues in Scots pine before a mortality event, while the starch-to-sugar ratios did not change during a milder and non-lethal drought (Schönbeck et al., 2020). The use of local storage for osmotic regulation thus seems to be an indicator of carbon starvation and does enable survival under extreme drought. If plants indeed increase the concentrations of soluble sugars to maintain turgor under declining water potentials, the NSC depletion often seen in dying trees (Adams et al., 2017) is likely to act as an underlying cause of hydraulic failure rather than a separate process. This direct link between the two processes may explain the often-divergent explanations of the proximate causes of plant death under drought.

4.2 | Tree size effects

The observed positive effect of tree height on survival contrasts with the mounting evidence that larger trees tend to be more susceptible to drought-induced mortality across biomes (Bennett et al., 2015; O'Brien et al., 2017; Stovall et al., 2019), although some authors report opposite patterns (van Mantgem et al., 2009; Nolan et al., 2021; Peng et al., 2011). Notably, most studies reporting a positive association between tree size and mortality focused on adult trees in mature forest stands. Under these conditions, crown exposure (Stovall et al., 2019) and path length-related constraints on water transport (Ryan & Yoder, 1997) are likely more relevant. Our analysis, in turn, focused on densely spaced young trees (planted in 2013 at the age of 1–3 years) with limited variation in height (Table 1).

Under these circumstances, negative density-dependent drivers of mortality are likely to dominate (Crouchet et al., 2019), disproportionately affecting smaller, competitively suppressed individuals via self- and alien-thinning (Kohyama, 1994). Meanwhile, the larger trees in the experiment may have possessed a competitive advantage due to their extensive root system and better access to deeper soil water, particularly during periods of water shortage (Song et al., 2018; Yanai et al., 2006).

4.3 | Bark beetle effects on conifers

The observed strongly elevated mortality risk for trees infested with bark beetles is consistent with a drought-driven predisposition for biotic attacks (McDowell et al., 2011). A potential decline in resin exudation and thus defense capability caused by the reduction of relative tissue water content made *P. abies* vulnerable to insect infestation (Netherer et al., 2015). As bark beetles cause physical damage to the phloem and xylem surface that is likely to affect both carbon metabolism and xylem water transport, their role for plant death cannot be understood without acknowledging its link to other processes driving drought-induced mortality (Trugman et al., 2021). Because trees also died in large numbers without visible signs of beetle infestation during the drought event, while a number of infested trees were able to survive, biotic attack is unlikely to be the main driver of mortality in the affected species. Rather, we assume that pest infestation acts as an additional stressor amplifying the risk of death by other causes.

Neighborhood effects can profoundly impact the predisposition to insect herbivore (Berthelot et al., 2021; Castagneyrol et al., 2018). The comparatively low influence of the presence of infested neighbor trees in our study may be related to the timing of the assessment of pest infestation in late 2018. At this time, the drought and associated insect outbreaks had probably already run their course and further spread was unlikely.

4.4 | Nutrient and environmental effects

Limitations posed by the design of the IDENT experiment preclude a clear interpretation of the nutrient effects, as fertilizer was only applied to the subset of European species and several highly relevant species-level traits were only measured on the control treatment. So far, only a limited number of studies are available for the interaction between drought and plant nutrition and the role of nutrients in drought-induced tree mortality (Gessler et al., 2017; Royo & Knight, 2012; Sargent et al., 2014). However, fertilization can reasonably be assumed to affect tree size, hydraulic efficiency and safety (Zhang et al., 2018), carbon dynamics (Li et al., 2018; Schönbeck et al., 2021) and susceptibility to bark beetles (Herms, 2002), as well as other potential unmeasured predictors of mortality. The main rationale for including nutrient effects in our model was therefore not to accurately estimate their total effect

on mortality, but to control for potential confounding effects (see Supplementary Material S1).

Although we observed no direct effect of the abiotic environment of trees via the fertilization treatment, our analysis of plot-specific effects on mortality (Figure S2.6) provides evidence that the individual mortality risk was modulated by small-scale environmental differences. The exact cause of these plot-specific differences is unknown, but they had a non-negligible contribution to the total variance in mortality risk, which may be associated with differences, for example, in soil texture, rooting depth, or wind exposition.

4.5 | Neighborhood interactions

High neighborhood tree species diversity might help to mitigate drought impacts due to complementarity effects, that is, temporal or spatial resource partitioning that results in higher water availability in mixed than in pure communities, or facilitation, that is, a positive effect on the functioning of cohabiting species by, for example, hydraulic redistribution (Grossiord, 2019). According to our model, neighborhood interspecific interactions played an important role for the survival of trees, either mitigating or enhancing drought effects depending on the surrounding species. The species-specificity of the interactions may explain controversial reports of species-mixing effects on drought effects (Fichtner et al., 2020; Grossiord, 2019; Schnabel et al., 2019).

The increased survival of trees with neighbor species that suffered extreme losses may be a result of competitive release, especially in the case of *Larix* spp. and *Betula* spp., which did not compete for water after their early leaf shedding in 2018. However, having larger neighbors was beneficial for the survival not only for the neighbors of trees belonging to these two species, but in the majority of species combinations (Figure 5). This indicates that notwithstanding the dense planting grid in the IDENT experiment, the shelter from wind and insolation provided by larger trees in most species combinations had a stronger effect on the survival of their neighbors than the more intense competition for water, a finding that may have important repercussions for management decisions for reforestation programs and plantations.

Another important implication of our model is that drought-related interactions between neighboring trees are directed and species-specific. Although similar patterns have been described for adult trees (Forrester et al., 2016), to our knowledge our study is the first to develop a formal model for the effect of all possible inter- and intraspecific neighborhood interactions on mortality risk on the individual level. Studies of mitigation and competition tend to focus on the effect of aggregate measures of diversity, such as species richness (e.g., Vitali et al., 2018) or functional diversity (e.g., Gazol & Camarero, 2016). These measures integrate over all possible neighborhood interactions and sacrifice information on the individual level, which is the scale on which processes affecting survival can be expected to act (Clark et al., 2011). Shifting the focus on the

individual level reveals that a net positive effect of diversity on survival can only occur if interspecific neighborhood interactions are on average more beneficial than intraspecific interactions, which is a testable assumption in our model. Whether this is the case fundamentally depends on the species sample, which may result in contradictory findings especially when studies comprise low numbers of species. Methods that preserve the information about the identity of interacting species allow for a more nuanced understanding of the underlying processes and provide valuable additional information that, for example, permits the identification of mutually beneficial species combinations, a precondition for establishing drought-resistant forest stands and commercial tree plantations.

5 | CONCLUSIONS

The extreme natural drought event in 2018 that killed over one third of the trees at the IDENT tree diversity experiment in Freiburg, Germany, provided a unique opportunity to compare the mutually inclusive mechanisms underlying drought-induced mortality in a unified setting. Given the projected increase in drought exposure in most of the world's forested biomes and the increase in disturbed areas that need to be afforested, improving the mechanistic understanding of processes involved in drought-induced tree mortality at young age is essential for afforestation success. Specifically, there is a need for an improved understanding of the complex processes that link carbohydrate metabolism and water relations, and the ways mortality risk is modulated by pests, environmental conditions, and neighborhood interactions among trees varying in size and species composition in a non-zero-sum list of effects. Our results support the assumption that severe tissue dehydration caused by hydraulic failure marks the final stage in the process of tree death under drought. However, although hydraulic traits are closely associated with species-specific drought responses, they are most likely not sufficient to predict individual mortality risk. Instead, the individual probability of reaching lethal desiccation thresholds depends on a series of mutually inclusive processes, notably starch depletion and conversion into soluble sugars, which are known to be important for osmotic adjustment, and close neighborhood composition.

CODE AVAILABILITY STATEMENT

The code for data processing and for fitting the model described in S1 is a part of a digital supplement that is available under https://github.com/r-link/mutually_inclusive_mechanisms along with the data.

ACKNOWLEDGEMENTS

We thank C. Gernert, Y. Heppenstiel, B. Kukatsch, S. Ouyang, and L. Schönbeck for their support in the laboratories and S. Bilodeau-Gauthier, A. Böminghaus, G. Csapek, A.-L. Hillebrecht, A. Klingler, D. Saito, A. Schäfer, D. Sprenger, M. Romer, M. Ulmerich, J. Maron, and M. Witt for their contribution to data collection at IDENT Freiburg. Funding by the German Research Foundation (DFG 384026712

to L.R.; DFG 316733524 to C.A.N.) and the University of Freiburg (Innovationsfonds Forschung to M.S.-L. and J.B.) is gratefully acknowledged. A.G. and M.S. acknowledge support from the Swiss Science Foundation (SNF 310030, 189109). We further acknowledge the constructive and helpful comments of two reviewers. The research presented here contributes to the International Tree Mortality Network (<https://www.tree-mortality.net/>), an initiative of the IUFRO Task Force on Tree Mortality (<https://www.iufro.org/science/task-forces/tree-mortality-patterns/>), and to the Global Network of Tree Diversity Experiments (TreeDivNet; <https://treedivnet.ugent.be/>), belonging to the IDENT network within TreeDivNet. Open access funding enabled and organized by ProjektDEAL.

CONFLICT OF INTEREST

The authors declare no competing interests.

AUTHOR CONTRIBUTION

A.P. and C.M. developed the original IDENT design. M.S.-L. and J.B. expanded and implemented the design for the Freiburg trial and maintained it together with C.A.N. and T.G., L.R., B.S., and A.G. developed the presented study. C.A.N. was responsible for pre-drought inventories, P.H. performed the mortality inventory and field sampling with support from L.R., and K.K. provided drone derived tree heights. P.H. performed all physiological measurements with support from M.S., R.M.L. developed the model and performed the statistical analyses, and P.H., R.M.L., and B.S. wrote the first version of the manuscript, which was intensively discussed and revised by all authors.

DATA AVAILABILITY STATEMENT

The full data set used for model fitting is a part of a digital supplement that is available as a Github repository https://github.com/r-link/mutually_inclusive_mechanisms. The raw data are further deposited at <https://doi.org/10.5061/dryad.sqv9s4n5t>.

ORCID

Peter Hajek  <https://orcid.org/0000-0001-5268-8917>
 Roman M. Link  <https://orcid.org/0000-0003-0588-3757>
 Charles A. Nock  <https://orcid.org/0000-0002-3483-0390>
 Jürgen Bauhus  <https://orcid.org/0000-0002-9673-4986>
 Tobias Gebauer  <https://orcid.org/0000-0003-2751-4071>
 Arthur Gessler  <https://orcid.org/0000-0002-1910-9589>
 Kyle Kovach  <https://orcid.org/0000-0002-1498-6363>
 Alain Paquette  <https://orcid.org/0000-0003-1048-9674>
 Matthias Saurer  <https://orcid.org/0000-0002-3954-3534>
 Michael Scherer-Lorenzen  <https://orcid.org/0000-0001-9566-590X>
 Laura Rose  <https://orcid.org/0000-0003-4523-4145>
 Bernhard Schuldt  <https://orcid.org/0000-0003-4738-5289>

REFERENCES

Adams, H. D., Zeppel, M. J. B., Anderegg, W. R. L., Hartmann, H., Landhäusser, S. M., Tissue, D. T., Huxman, T. E., Hudson, P. J.,

Franz, T. E., Allen, C. D., Anderegg, L. D. L., Barron-Gafford, G. A., Beerling, D. J., Breshears, D. D., Brodrigg, T. J., Bugmann, H., Cobb, R. C., Collins, A. D., Dickman, L. T., ... McDowell, N. G. (2017). A multi-species synthesis of physiological mechanisms in drought-induced tree mortality. *Nature Ecology & Evolution*, 1(9), 1285–1291. <https://doi.org/10.1038/s41559-017-0248-x>

Allen, C. D., Breshears, D. D., & McDowell, N. G. (2015). On underestimation of global vulnerability to tree mortality and forest die-off from hotter drought in the Anthropocene. *Ecosphere*, 6(8), art129. <https://doi.org/10.1890/ES15-00203.1>

Ammer, C. (2019). Diversity and forest productivity in a changing climate. *New Phytologist*, 221(1), 50–66. <https://doi.org/10.1111/nph.15263>

Anderegg, W. R. L., Klein, T., Bartlett, M., Sack, L., Pellegrini, A. F. A., Choat, B., & Jansen, S. (2016). Meta-analysis reveals that hydraulic traits explain cross-species patterns of drought-induced tree mortality across the globe. *Proceedings of the National Academy of Sciences*, 113(18), 5024–5029. <https://doi.org/10.1073/pnas.1525678113>

Bennett, A. C., McDowell, N. G., Allen, C. D., & Anderson-Teixeira, K. J. (2015). Larger trees suffer most during drought in forests worldwide. *Nature Plants*, 1(10), 15139. <https://doi.org/10.1038/nplants.2015.139>

Berthelot, S., Fröhbrodt, T., Hajek, P., Nock, C. A., Dormann, C. F., Bauhus, J., & Fründ, J. (2021). Tree diversity reduces the risk of bark beetle infestation for preferred conifer species, but increases the risk for less preferred hosts. *Journal of Ecology*, 109(7), 2649–2661. <https://doi.org/10.1111/1365-2745.13672>

Blackman, C. J., Creek, D., Maier, C., Aspinwall, M. J., Drake, J. E., Pfautsch, S., O'Grady, A., Delzon, S., Medlyn, B. E., Tissue, D. T., & Choat, B. (2019a). Drought response strategies and hydraulic traits contribute to mechanistic understanding of plant dry-down to hydraulic failure. *Tree Physiology*, 39(6), 910–924. <https://doi.org/10.1093/treephys/tpz016>

Blackman, C. J., Li, X., Choat, B., Rymer, P. D., Kauwe, M. G. D., Duursma, R. A., Tissue, D. T., & Medlyn, B. E. (2019b). Desiccation time during drought is highly predictable across species of *Eucalyptus* from contrasting climates. *New Phytologist*, 224(2), 632–643. <https://doi.org/10.1111/nph.16042>

Blackman, C. J., Pfautsch, S., Choat, B., Delzon, S., Gleason, S. M., & Duursma, R. A. (2016). Toward an index of desiccation time to tree mortality under drought. *Plant, Cell & Environment*, 39(10), 2342–2345. <https://doi.org/10.1111/pce.12758>

Brodrigg, T. J., & Cochard, H. (2009). Hydraulic failure defines the recovery and point of death in water-stressed conifers. *Plant Physiology*, 149(1), 575–584. <https://doi.org/10.1104/pp.108.129783>

Brodrigg, T. J., Powers, J., Cochard, H., & Choat, B. (2020). Hanging by a thread? *Forests and Drought*. *Science*, 368(6488), 261–266. <https://doi.org/10.1126/science.aat7631>

Cailleret, M., Jansen, S., Robert, E. M. R., Desoto, L., Aakala, T., Antos, J. A., Beikircher, B., Bigler, C., Bugmann, H., Caccianiga, M., Čada, V., Camarero, J. J., Cherubini, P., Cochard, H., Coyea, M. R., Čufar, K., Das, A. J., Davi, H., Delzon, S., ... Martínez-Vilalta, J. (2017). A synthesis of radial growth patterns preceding tree mortality. *Global Change Biology*, 23(4), 1675–1690. <https://doi.org/10.1111/gcb.13535>

Carminati, A., & Javaux, M. (2020). Soil rather than xylem vulnerability controls stomatal response to drought. *Trends in Plant Science*, 25(9), 868–880. <https://doi.org/10.1016/j.tplants.2020.04.003>

Carpenter, B., Gelman, A., Hoffman, M. D., Lee, D., Goodrich, B., Betancourt, M., Brubaker, M., Guo, J., Li, P., & Riddell, A. (2017). Stan: A probabilistic programming language. *Journal of Statistical Software*, 76(1). <https://doi.org/10.18637/jss.v076.i01>

Castagneyrol, B., Jactel, H., & Moreira, X. (2018). Anti-herbivore defences and insect herbivory: Interactive effects of drought and tree neighbours. *Journal of Ecology*, 106(5), 2043–2057. <https://doi.org/10.1111/1365-2745.12956>

- Charrier, G., Torres-Ruiz, J. M., Badel, E., Burlett, R., Choat, B., Cochard, H., Delmas, C. E. L., Domec, J.-C., Jansen, S., King, A., Lenoir, N., Martin-StPaul, N., Gambetta, G. A., & Delzon, S. (2016). Evidence for hydraulic vulnerability segmentation and lack of xylem refill during under tension. *Plant Physiology*, 172(3), 1657–1668. <https://doi.org/10.1104/pp.16.01079>
- Choat, B., Brodribb, T. J., Brodersen, C. R., Duursma, R. A., López, R., & Medlyn, B. E. (2018). Triggers of tree mortality under drought. *Nature*, 558(7711), 531–539. <https://doi.org/10.1038/s41586-018-0240-x>
- Choat, B., Nolf, M., López, R., Peters, J. M. R., Carins-Murphy, M. R., Creek, D., & Brodribb, T. J. (2019). Non-invasive imaging shows no evidence of embolism repair after drought in tree species of two genera. *Tree Physiology*, 39(1), 113–121. <https://doi.org/10.1093/treephys/tpy093>
- Clark, J. S., Bell, D. M., Hersh, M. H., Kwit, M. C., Moran, E., Salk, C., Stine, A., Valle, D., & Zhu, K. (2011). Individual-scale variation, species-scale differences: Inference needed to understand diversity. *Ecology Letters*, 14(12), 1273–1287. <https://doi.org/10.1111/j.1461-0248.2011.01685.x>
- Cochard, H., Damour, G., Bodet, C., Tharwat, I., Poirier, M., & Améglio, T. (2005). Evaluation of a new centrifuge technique for rapid generation of xylem vulnerability curves. *Physiologia Plantarum*, 124(4), 410–418. <https://doi.org/10.1111/j.1399-3054.2005.00526.x>
- Crouchet, S. E., Jensen, J., Schwartz, B. F., & Schwinning, S. (2019). Tree mortality after a hot drought: Distinguishing density-dependent and independent drivers and why it matters. *Frontiers in Forests and Global Change*, 2, 21. <https://doi.org/10.3389/ffgc.2019.00021>
- Dai, A. (2013). Increasing drought under global warming in observations and models. *Nature Climate Change*, 3(1), 52–58. <https://doi.org/10.1038/nclimate1633>
- de la Mata, R., Hood, S., & Sala, A. (2017). Insect outbreak shifts the direction of selection from fast to slow growth rates in the long-lived conifer *Pinus ponderosa*. *Proceedings of the National Academy of Sciences*, 114(28), 7391–7396. <https://doi.org/10.1073/pnas.1700032114>
- DWD Climate Data Center—CDC. (2020). Daily station observations precipitation height in mm and mean temperature at 2 m above ground in °C for Germany.
- Fichtner, A., Schnabel, F., Bruehlheide, H., Kunz, M., Mausolf, K., Schuldt, A., Härdtle, W., & Oheimb, G. (2020). Neighbourhood diversity mitigates drought impacts on tree growth. *Journal of Ecology*, 108(3), 865–875. <https://doi.org/10.1111/1365-2745.13353>
- Forrester, D. I., Bonal, D., Dawud, S., Gessler, A., Granier, A., Pollastrini, M., & Grossiord, C. (2016). Drought responses by individual tree species are not often correlated with tree species diversity in European forests. *Journal of Applied Ecology*, 53(6), 1725–1734. <https://doi.org/10.1111/1365-2664.12745>
- Gazol, A., & Camarero, J. J. (2016). Functional diversity enhances silver fir growth resilience to an extreme drought. *Journal of Ecology*, 104(4), 1063–1075. <https://doi.org/10.1111/1365-2745.12575>
- Gessler, A., Schaub, M., & McDowell, N. G. (2017). The role of nutrients in drought-induced tree mortality and recovery. *New Phytologist*, 214(2), 513–520. <https://doi.org/10.1111/nph.14340>
- Grossiord, C. (2019). Having the right neighbours: How tree species diversity modulates drought impacts on forests. *New Phytologist*, 228(1), 42–49. <https://doi.org/10.1111/nph.15667>
- Guadagno, C. R., Ewers, B. E., Speckman, H. N., Aston, T. L., Huhn, B. J., DeVore, S. B., Ladwig, J. T., Strawn, R. N., & Weinig, C. (2017). Dead or alive? Using membrane failure and chlorophyll a fluorescence to predict plant mortality from drought. *Plant Physiology*, 175(1), 223–234. <https://doi.org/10.1104/pp.16.00581>
- Hammond, W. M., Williams, A. P., Abatzoglou, J. T., Adams, H. D., Klein, T., López Rodríguez, R., Sáenz-Romero, C., Hartmann, H., Breshears, D. D., & Allen, C. D. (2022). Global field observations of tree die-off reveal hotter-drought fingerprint for Earth's forests. *Nature Communications*.
- Hart, S. J., Veblen, T. T., Eisenhart, K. S., Jarvis, D., & Kulakowski, D. (2014). Drought induces spruce beetle (*Dendroctonus rufipennis*) outbreaks across northwestern Colorado. *Ecology*, 95(4), 930–939. <https://doi.org/10.1890/13-0230.1>
- Hartmann, H., Link, R. M., & Schuldt, B. (2021). A whole-plant perspective of isohydry: Stem-level support for leaf-level plant water regulation. *Tree Physiology*, 41(6), 901–905. <https://doi.org/10.1093/treephys/tpab011>
- Hartmann, H., Ziegler, W., Kolbe, O., & Trumbore, S. (2013). Thirst beats hunger—Declining hydration during drought prevents carbon starvation in Norway spruce saplings. *New Phytologist*, 200(2), 340–349. <https://doi.org/10.1111/nph.12331>
- He, W., Liu, H., Qi, Y., Liu, F., & Zhu, X. (2020). Patterns in nonstructural carbohydrate contents at the tree organ level in response to drought duration. *Global Change Biology*, 26(6), 3627–3638. <https://doi.org/10.1111/gcb.15078>
- Hegyi, F. (1974). A simulation model for managing jack-pine stands. In J. Fries (Ed.), *Growth models for tree and stand simulation*, Vol. 30 (pp. 74–90). Royal College of Forestry.
- Hermes, D. A. (2002). Effects of fertilization on insect resistance of woody ornamental plants: Reassessing an entrenched paradigm. *Environmental Entomology*, 31(6), 923–933. <https://doi.org/10.1603/0046-225X-31.6.923>
- Herrero, A., Castro, J., Zamora, R., Delgado-Huertas, A., & Querejeta, J. I. (2013). Growth and stable isotope signals associated with drought-related mortality in saplings of two coexisting pine species. *Oecologia*, 173(4), 1613–1624. <https://doi.org/10.1007/s00442-013-2707-7>
- Hoch, G., Popp, M., & Körner, C. (2002). Altitudinal increase of mobile carbon pools in *Pinus cembra* suggests sink limitation of growth at the Swiss treeline. *Oikos*, 98(3), 361–374. <https://doi.org/10.1034/j.1600-0706.2002.980301.x>
- Huang, J., Kautz, M., Trowbridge, A. M., Hammerbacher, A., Raffa, K. F., Adams, H. D., Goodsman, D. W., Xu, C., Meddens, A. J. H., Kandasamy, D., Gershenson, J., Seidl, R., & Hartmann, H. (2020). Tree defence and bark beetles in a drying world: Carbon partitioning, functioning and modelling. *New Phytologist*, 225(1), 26–36. <https://doi.org/10.1111/nph.16173>
- Kannenbergh, S. A., & Phillips, R. P. (2020). Non-structural carbohydrate pools not linked to hydraulic strategies or carbon supply in tree saplings during severe drought and subsequent recovery. *Tree Physiology*, 40(2), 259–271. <https://doi.org/10.1093/treephys/tpz132>
- Kohyama, T. (1994). Size-structure-based models of forest dynamics to interpret population- and community-level mechanisms. *Journal of Plant Research*, 107(1), 107–116. <https://doi.org/10.1007/BF02344537>
- Landhäusser, S. M., Chow, P. S., Dickman, L. T., Furze, M. E., Kuhlman, I., Schmid, S., Wiesenbauer, J., Wild, B., Gleixner, G., Hartmann, H., Hoch, G., McDowell, N. G., Richardson, A. D., Richter, A., & Adams, H. D. (2018). Standardized protocols and procedures can precisely and accurately quantify non-structural carbohydrates. *Tree Physiology*, 38(12), 1764–1778. <https://doi.org/10.1093/treephys/tpy118>
- Li, W., Hartmann, H., Adams, H. D., Zhang, H., Jin, C., Zhao, C., Guan, D., Wang, A., Yuan, F., & Wu, J. (2018). The sweet side of global change—dynamic responses of non-structural carbohydrates to drought, elevated CO₂ and nitrogen fertilization in tree species. *Tree Physiology*, 38(11), 1706–1723. <https://doi.org/10.1093/treephys/tpy059>
- Li, X., Piao, S., Wang, K., Wang, X., Wang, T., Ciais, P., Chen, A., Lian, X., Peng, S., & Peñuelas, J. (2020). Temporal trade-off between gymnosperm resistance and resilience increases forest sensitivity

- to extreme drought. *Nature Ecology & Evolution*, 4(8), 1075–1083. <https://doi.org/10.1038/s41559-020-1217-3>
- Lobo, A., Torres-Ruiz, J. M., Burlett, R., Lemaire, C., Parise, C., Francioni, C., Truffaut, L., Tomášková, I., Hansen, J. K., Kjær, E. D., Kremer, A., & Delzon, S. (2018). Assessing inter- and intraspecific variability of xylem vulnerability to embolism in oaks. *Forest Ecology and Management*, 424, 53–61. <https://doi.org/10.1016/j.foreco.2018.04.031>
- López, R., Cano, F. J., Martin-StPaul, N. K., Cochard, H., & Choat, B. (2021). Coordination of stem and leaf traits define different strategies to regulate water loss and tolerance ranges to aridity. *New Phytologist*, 230(2), 497–509. <https://doi.org/10.1111/nph.17185>
- Mantova, M., Menezes-Silva, P. E., Badel, E., Cochard, H., & Torres-Ruiz, J. M. (2021). The interplay of hydraulic failure and cell vitality explains tree capacity to recover from drought. *Physiologia Plantarum*, 172(1), 247–257. <https://doi.org/10.1111/ppl.13331>
- McDowell, N. G., Allen, C. D., Anderson-Teixeira, K., Aukema, B. H., Bond-Lamberty, B., Chini, L., Clark, J. S., Dietze, M., Grossiord, C., Hanbury-Brown, A., Hurr, G. C., Jackson, R. B., Johnson, D. J., Kueppers, L., Lichstein, J. W., Ogle, K., Poulter, B., Pugh, T. A. M., Seidl, R., ... Xu, C. (2020). Pervasive shifts in forest dynamics in a changing world. *Science*, 368(6494), eaz9463. <https://doi.org/10.1126/science.aaz9463>
- McDowell, N. G., Beerling, D. J., Breshears, D. D., Fisher, R. A., Raffa, K. F., & Stitt, M. (2011). The interdependence of mechanisms underlying climate-driven vegetation mortality. *Trends in Ecology & Evolution*, 26(10), 523–532. <https://doi.org/10.1016/j.tree.2011.06.003>
- McDowell, N. G., Brodribb, T. J., & Nardini, A. (2019). Hydraulics in the 21st century. *New Phytologist*, 224(2), 537–542. <https://doi.org/10.1111/nph.16151>
- McDowell, N., Pockman, W. T., Allen, C. D., Breshears, D. D., Cobb, N., Kolb, T., Plaut, J., Sperry, J., West, A., Williams, D. G., & Yeepez, E. A. (2008). Mechanisms of plant survival and mortality during drought: Why do some plants survive while others succumb to drought? *New Phytologist*, 178(4), 719–739. <https://doi.org/10.1111/j.1469-8137.2008.02436.x>
- McDowell, N. G., & Sevanto, S. (2010). The mechanisms of carbon starvation: How, when, or does it even occur at all? *The New Phytologist*, 186(2), 264–266. <https://doi.org/10.1111/j.1469-8137.2010.03232.x>
- Mencuccini, M., Minunno, F., Salmon, Y., Martínez-Vilalta, J., & Hölttä, T. (2015). Coordination of physiological traits involved in drought-induced mortality of woody plants. *New Phytologist*, 208(2), 396–409. <https://doi.org/10.1111/nph.13461>
- Netherer, S., Matthews, B., Katzensteiner, K., Blackwell, E., Henschke, P., Hietz, P., Pennerstorfer, J., Rosner, S., Kikuta, S., Schume, H., & Schopf, A. (2015). Do water-limiting conditions predispose Norway spruce to bark beetle attack? *New Phytologist*, 205(3), 1128–1141. <https://doi.org/10.1111/nph.13166>
- Nolan, R. H., Gauthey, A., Losso, A., Medlyn, B. E., Smith, R., Chhajer, S. S., Fuller, K., Song, M., Li, X., Beaumont, L. J., Boer, M. M., Wright, I. J., & Choat, B. (2021). Hydraulic failure and tree size linked with canopy die-back in eucalypt forest during extreme drought. *New Phytologist*, 230(4), 1354–1365. <https://doi.org/10.1111/nph.17298>
- O'Brien, M. J., Engelbrecht, B. M. J., Joswig, J., Pereyra, G., Schuldt, B., Jansen, S., Kattge, J., Landhäusser, S. M., Levick, S. R., Preisler, Y., Väänänen, P., & Macinnis-Ng, C. (2017). A synthesis of tree functional traits related to drought-induced mortality in forests across climatic zones. *Journal of Applied Ecology*, 54(6), 1669–1686. <https://doi.org/10.1111/1365-2664.12874>
- O'Brien, M. J., Valtat, A., Abiven, S., Studer, M. S., Ong, R., & Schmid, B. (2020). The role of soluble sugars during drought in tropical tree seedlings with contrasting tolerances. *Journal of Plant Ecology*, 13(4), 389–397. <https://doi.org/10.1093/jpe/rtaa017>
- Ogle, K., Barber, J. J., Willson, C., & Thompson, B. (2009). Hierarchical statistical modeling of xylem vulnerability to cavitation. *New Phytologist*, 182(2), 541–554. <https://doi.org/10.1111/j.1469-8137.2008.02760.x>
- Pantin, F., Fanciullino, A.-L., Massonnet, C., Dauzat, M., Simonneau, T., & Muller, B. (2013). Buffering growth variations against water deficits through timely carbon usage. *Frontiers in Plant Science*, 4, 483. <https://doi.org/10.3389/fpls.2013.00483>
- Paquette, A., Hector, A., Castagneyrol, B., Vanhellefont, M., Koricheva, J., Scherer-Lorenzen, M., & Verheyen, K. (2018). A million and more trees for science. *Nature Ecology & Evolution*, 2(5), 763–766. <https://doi.org/10.1038/s41559-018-0544-0>
- Peng, C., Ma, Z., Lei, X., Zhu, Q., Chen, H., Wang, W., Liu, S., Li, W., Fang, X., & Zhou, X. (2011). A drought-induced pervasive increase in tree mortality across Canada's boreal forests. *Nature Climate Change*, 1(9), 467–471. <https://doi.org/10.1038/nclimate1293>
- Peters, W., Bastos, A., Ciais, P., & Vermeulen, A. (2020). A historical, geographical and ecological perspective on the 2018 European summer drought. *Philosophical Transactions of the Royal Society B: Biological Sciences*, 375(1810), 20190505. <https://doi.org/10.1098/rstb.2019.0505>
- Powers, J. S., Vargas, G., Brodribb, T. J., Schwartz, N. B., Pérez-Aviles, D., Smith-Martin, C. M., Becknell, J. M., Aureli, F., Blanco, R., Calderón-Morales, E., Calvo-Alvarado, J. C., Calvo-Obando, A. J., Chavarria, M. M., Carvajal-Vanegas, D., Jiménez-Rodríguez, C. D., Murillo Chacon, E., Schaffner, C. M., Werden, L. K., Xu, X., & Medvigy, D. (2020). A catastrophic tropical drought kills hydraulically vulnerable tree species. *Global Change Biology*, 26(5), 3122–3133. <https://doi.org/10.1111/gcb.15037>
- R Core Team. (2020). *R: A language and environment for statistical computing*. R Foundation for Statistical Computing.
- Rehshuh, R., Cecilia, A., Zuber, M., Faragó, T., Baumbach, T., Hartmann, H., Jansen, S., Mayr, S., & Ruehr, N. (2020). Drought-induced xylem embolism limits the recovery of leaf gas exchange in Scots pine. *Plant Physiology*, 184(2), 852–864. <https://doi.org/10.1104/pp.20.00407>
- Royo, A. A., & Knight, K. S. (2012). White ash (*Fraxinus americana*) decline and mortality: The role of site nutrition and stress history. *Forest Ecology and Management*, 286, 8–15. <https://doi.org/10.1016/j.foreco.2012.08.049>
- Ryan, M. G., & Yoder, B. J. (1997). Hydraulic limits to tree height and tree growth. *BioScience*, 47(4), 235–242. <https://doi.org/10.2307/1313077>
- Sapes, G., Demaree, P., Lekberg, Y., & Sala, A. (2021). Plant carbohydrate depletion impairs water relations and spreads via ectomycorrhizal networks. *New Phytologist*, 229(6), 3172–3183. <https://doi.org/10.1111/nph.17134>
- Sapes, G., Roskilly, B., Dobrowski, S., Maneta, M., Anderegg, W. R. L., Martínez-Vilalta, J., & Sala, A. (2019). Plant water content integrates hydraulics and carbon depletion to predict drought-induced seedling mortality. *Tree Physiology*, 39(8), 1300–1312. <https://doi.org/10.1093/treephys/tpz062>
- Schnabel, F., Schwarz, J. A., Dănescu, A., Fichtner, A., Nock, C. A., Bauhus, J., & Potvin, C. (2019). Drivers of productivity and its temporal stability in a tropical tree diversity experiment. *Global Change Biology*, 25(12), 4257–4272. <https://doi.org/10.1111/gcb.14792>
- Schönbeck, L., Gessler, A., Schaub, M., Rigling, A., Hoch, G., Kahmen, A., & Li, M.-H. (2020). Soil nutrients and lowered source:sink ratio mitigate effects of mild but not of extreme drought in trees. *Environmental and Experimental Botany*, 169, 103905. <https://doi.org/10.1016/j.envexpbot.2019.103905>
- Schönbeck, L., Li, M.-H., Lehmann, M. M., Rigling, A., Schaub, M., Hoch, G., Kahmen, A., & Gessler, A. (2021). Soil nutrient availability alters tree carbon allocation dynamics during drought. *Tree Physiology*, 41(5), 697–707. <https://doi.org/10.1093/treephys/tpaa139>
- Schuldt, B., Buras, A., Arend, M., Vitasse, Y., Beierkuhnlein, C., Damm, A., Gharun, M., Grams, T. E. E., Hauck, M., Hajek, P., Hartmann, H.,

- Hiltbrunner, E., Hoch, G., Holloway-Phillips, M., Körner, C., Larysch, E., Lütke, T., Nelson, D. B., Rammig, A., ... Kahmen, A. (2020). A first assessment of the impact of the extreme 2018 summer drought on Central European forests. *Basic and Applied Ecology*, 45, 86–103. <https://doi.org/10.1016/j.baae.2020.04.003>
- Seidl, R., Thom, D., Kautz, M., Martin-Benito, D., Peltoniemi, M., Vacchiano, G., Wild, J., Ascoli, D., Petr, M., Honkaniemi, J., Lexer, M. J., Trotsiuk, V., Mairota, P., Svoboda, M., Fabrika, M., Nagel, T. A., & Reyer, C. P. O. (2017). Forest disturbances under climate change. *Nature Climate Change*, 7(6), 395–402. <https://doi.org/10.1038/nclimate3303>
- Sergent, A.-S., Rozenberg, P., & Bréda, N. (2014). Douglas-fir is vulnerable to exceptional and recurrent drought episodes and recovers less well on less fertile sites. *Annals of Forest Science*, 71(6), 697–708. <https://doi.org/10.1007/s13595-012-0220-5>
- Sevanto, S., McDowell, N. G., Dickman, L. T., Pangle, R., & Pockman, W. T. (2014). How do trees die? A test of the hydraulic failure and carbon starvation hypotheses. *Plant, Cell & Environment*, 37(1), 153–161. <https://doi.org/10.1111/pce.12141>
- Song, X., Gao, X., Dyck, M., Zhang, W., Wu, P., Yao, J., & Zhao, X. (2018). Soil water and root distribution of apple tree (*Malus pumila* Mill) stands in relation to stand age and rainwater collection and infiltration system (RWCI) in a hilly region of the Loess Plateau, China. *Catena*, 170, 324–334. <https://doi.org/10.1016/j.catena.2018.06.026>
- Stan Development Team. (2020). *RStan: The R interface to Stan*.
- Stovall, A. E. L., Shugart, H., & Yang, X. (2019). Tree height explains mortality risk during an intense drought. *Nature Communications*, 10(1), 4385. <https://doi.org/10.1038/s41467-019-12380-6>
- Thalmann, M., & Santelia, D. (2017). Starch as a determinant of plant fitness under abiotic stress. *New Phytologist*, 214(3), 943–951. <https://doi.org/10.1111/nph.14491>
- Tobner, C. M., Paquette, A., Reich, P. B., Gravel, D., & Messier, C. (2014). Advancing biodiversity–ecosystem functioning science using high-density tree-based experiments over functional diversity gradients. *Oecologia*, 174(3), 609–621. <https://doi.org/10.1007/s00442-013-2815-4>
- Tomasella, M., Casolo, V., Natale, S., Petruzzellis, F., Kofler, W., Beikircher, B., Mayr, S., & Nardini, A. (2021). Shade-induced reduction of stem nonstructural carbohydrates increases xylem vulnerability to embolism and impedes hydraulic recovery in *Populus nigra*. *New Phytologist*, 231(1), 108–121. <https://doi.org/10.1111/nph.17384>
- Trugman, A. T., Anderegg, L. D. L., Anderegg, W. R. L., Das, A. J., & Stephenson, N. L. (2021). Why is tree drought mortality so hard to predict? *Trends in Ecology & Evolution*, 36(6), 520–532. <https://doi.org/10.1016/j.tree.2021.02.001>
- Trugman, A. T., Detto, M., Bartlett, M. K., Medvigy, D., Anderegg, W. R. L., Schwalm, C., Schaffer, B., & Pacala, S. W. (2018). Tree carbon allocation explains forest drought-kill and recovery patterns. *Ecology Letters*, 21(10), 1552–1560. <https://doi.org/10.1111/ele.13136>
- Urli, M., Porte, A. J., Cochard, H., Guengant, Y., Burlett, R., & Delzon, S. (2013). Xylem embolism threshold for catastrophic hydraulic failure in angiosperm trees. *Tree Physiology*, 33(7), 672–683. <https://doi.org/10.1093/treephys/tpt030>
- van Mantgem, P. J., Stephenson, N. L., Byrne, J. C., Daniels, L. D., Franklin, J. F., Fule, P. Z., Harmon, M. E., Larson, A. J., Smith, J. M., Taylor, A. H., & Veblen, T. T. (2009). Widespread increase of tree mortality rates in the western United States. *Science*, 323(5913), 521–524. <https://doi.org/10.1126/science.1165000>
- Vitali, V., Forrester, D. I., & Bauhus, J. (2018). Know your neighbours: Drought response of Norway Spruce, Silver Fir and Douglas Fir in mixed forests depends on species identity and diversity of tree neighbourhoods. *Ecosystems*, 21(6), 1215–1229. <https://doi.org/10.1007/s10021-017-0214-0>
- Wein, A., Bauhus, J., Bilodeau-Gauthier, S., Scherer-Lorenzen, M., Nock, C., & Staab, M. (2016). Tree species richness promotes invertebrate herbivory on congeneric native and exotic tree saplings in a young diversity experiment. *PLoS One*, 11(12), e0168751. <https://doi.org/10.1371/journal.pone.0168751>
- Wong, S.-C. (1990). Elevated atmospheric partial-pressure of CO₂ and plant-growth. II: Nonstructural carbohydrate content in cotton plants and its effect on growth-parameters. *Photosynthesis Research*, 23, 171–180. <https://doi.org/10.1007/BF00035008>
- Yanai, R. D., Park, B. B., & Hamburg, S. P. (2006). The vertical and horizontal distribution of roots in northern hardwood stands of varying age. *Canadian Journal of Forest Research*, 36(2), 450–459. <https://doi.org/10.1139/x05-254>
- Young, D. J. N., Meyer, M., Estes, B., Gross, S., Wuenschel, A., Restaino, C., & Safford, H. D. (2020). Forest recovery following extreme drought in California, USA: Natural patterns and effects of pre-drought management. *Ecological Applications*, 30(1), e02002. <https://doi.org/10.1002/eap.2002>
- Yuan, W., Zheng, Y. I., Piao, S., Ciais, P., Lombardozzi, D., Wang, Y., Ryu, Y., Chen, G., Dong, W., Hu, Z., Jain, A. K., Jiang, C., Kato, E., Li, S., Lienert, S., Liu, S., Nabel, J. E. M. S., Qin, Z., Quine, T., ... Yang, S. (2019). Increased atmospheric vapor pressure deficit reduces global vegetation growth. *Science Advances*, 5(8), eaax1396. <https://doi.org/10.1126/sciadv.aax1396>
- Zhang, H., Li, W., Adams, H. D., Wang, A., Wu, J., Jin, C., Guan, D., & Yuan, F. (2018). Responses of woody plant functional traits to nitrogen addition: A meta-analysis of leaf economics, gas exchange, and hydraulic traits. *Frontiers in Plant Science*, 9, 683. <https://doi.org/10.3389/fpls.2018.00683>

SUPPORTING INFORMATION

Additional supporting information may be found in the online version of the article at the publisher's website.

How to cite this article: Hajek, P., Link, R. M., Nock, C. A., Bauhus, J., Gebauer, T., Gessler, A., Kovach, K., Messier, C., Paquette, A., Saurer, M., Scherer-Lorenzen, M., Rose, L., & Schuldt, B. (2022). Mutually inclusive mechanisms of drought-induced tree mortality. *Global Change Biology*, 28, 3365–3378. <https://doi.org/10.1111/gcb.16146>